Geofísica Internacional (1996), Vol. 35, Num. 3, pp. 301-314

Shear wave velocities beneath the eastern part of Brazil

Jorge Luis de Souza
Observatório Nacional, Departamento de Geofísica, Rio de Janeiro, Brasil.

RESUMEN

El perfil de velocidades de ondas S bajo Brasil Oriental fue obtenido de datos de dispersión de ondas de Rayleigh para 17 sismos con epicentro en el Atlántico Norte. La inversión sugiere una estructura de tres capas con velocidades de S de 3.30-3.57 km/s, 3.52-3.66 km/s y 3.86-3.92 km/s. Bajo el Moho se encuentran velocidades de 4.41-4.43 km/s. Algunas variaciones se discuten para cada una de las trayectorias. El modelo sugerido es similar a modelos anteriores para Sudamérica y Antártica.

PALABRAS CLAVE: Dispersión de ondas de Rayleigh, velocidad de ondas S, Brasil Oriental.

ABSTRACT

Rayleigh wave dispersion curves from seventeen earthquakes which occurred in the North Atlantic Ocean area are used to obtain the shear wave velocity structure of the eastern part of the Brazilian territory. The dispersion curves were divided into three groups of paths (A, B, and C) according to geographical position of the epicenters, and a dispersion curve representative of each path was computed. The inversion results of these dispersion curves show that the crustal structure is composed basically of three layers with S-wave velocities varying from 3.30-3.57 km/s, 3.52-3.66 km/s and 3.86-3.92 km/s, respectively. The sub-Moho layer is characterized by shear wave velocities varying from 4.41 to 4.43 km/s. Path C exhibits a sub-Moho thickness thinner than the other two paths. Below the sub-Moho layer, shear wave velocities of 4.27 km/s and 4.22 km/s are found in both paths A and C, but it has been clearly resolved only in path C where the S-wave velocity was assumed to be 4.22 km/s. A comparative analysis between the models obtained in the present study and those representative of other shield areas reveals a strong similarity between the models of eastern Brazil and those of eastern South America (Hwang and Mitchell, 1987) and Antarctica (Dewart and Toksoz, 1965; Singh, 1994). This is probably related to the past existence of Gondwanaland.

KEY WORDS: Rayleigh wave dispersion, shear wave velocity, Eastern Brazil.

INTRODUCTION

In contrast to the western part of the South American continent where it is possible to observe a high level of seismicity, the Brazilian territory is located in an intraplate region which is characterized by very low seismicity. The poor quantity, quality, and distribution of the seismological stations, either in Brazil or in the other countries of South America, have been the principal elements responsible for the limited knowledge of the Earth's interior in the area.

The recent installation of modern instrumentation (broad-band seismometers from IRIS, GEOSCOPE and GEOFON projects) at some sites of the WWSS network, as well as the future installation of new seismological stations in the South American region, several of these in the Brazilian territory, will allow for the development of many relevant seismological investigations concerning the Earth's constitution in the area and the planet's evolution as a whole.

The principal objective of this paper is to determine the shear wave velocity structure for the eastern part of Brazil from Rayleigh wave dispersion curves obtained at the Brazilian seismological station RDJ (Rio de Janeiro).

DATA PROCESSING

In order to study the eastern part of Brazil using data from the RDJ seismological station, it was necessary to use records from earthquakes which occurred in the North Atlantic Ocean. Using this criterion, seventeen surface wave records were selected. The location of both station and epicenters, as well as Rayleigh wave paths are shown in Figure 1. The hypocentral parameters (Table 1) were obtained from Earthquake Data Report Bulletins of USGS (United States Geological Survey).

The RDJ seismological station is composed of three long-period seismometers, one Sprengnether vertical long-period seismometer ($T_s \approx 15s$) and two Press-Ewing horizontal long-period seismometers ($T_s \approx 15s$), connected to galvanometers ($T_g \approx 80s$). Since 1978, when Observatório Nacional assumed the responsibility of station RDJ, this system produced analog records on photographic paper. Currently, a Teledyne Geotech, three-channel Helicorder recorder is being used to obtain analog records.

The vertical component of motion was used in this study. The seismograms were analyzed in order to identify the beginning of the Rayleigh waves and a time window for digitization was defined. These time windows were hand digitized at irregular intervals. A sampling interval of 1s was obtained after linear interpolation. An instrumental correction was applied during the determination of the source-station Rayleigh wave dispersion curves.

DETERMINATION OF CONTINENTAL DISPERSION CURVES

As observed in Figure 1, the source-station Rayleigh wave paths are composed of mixed paths, and, therefore, to

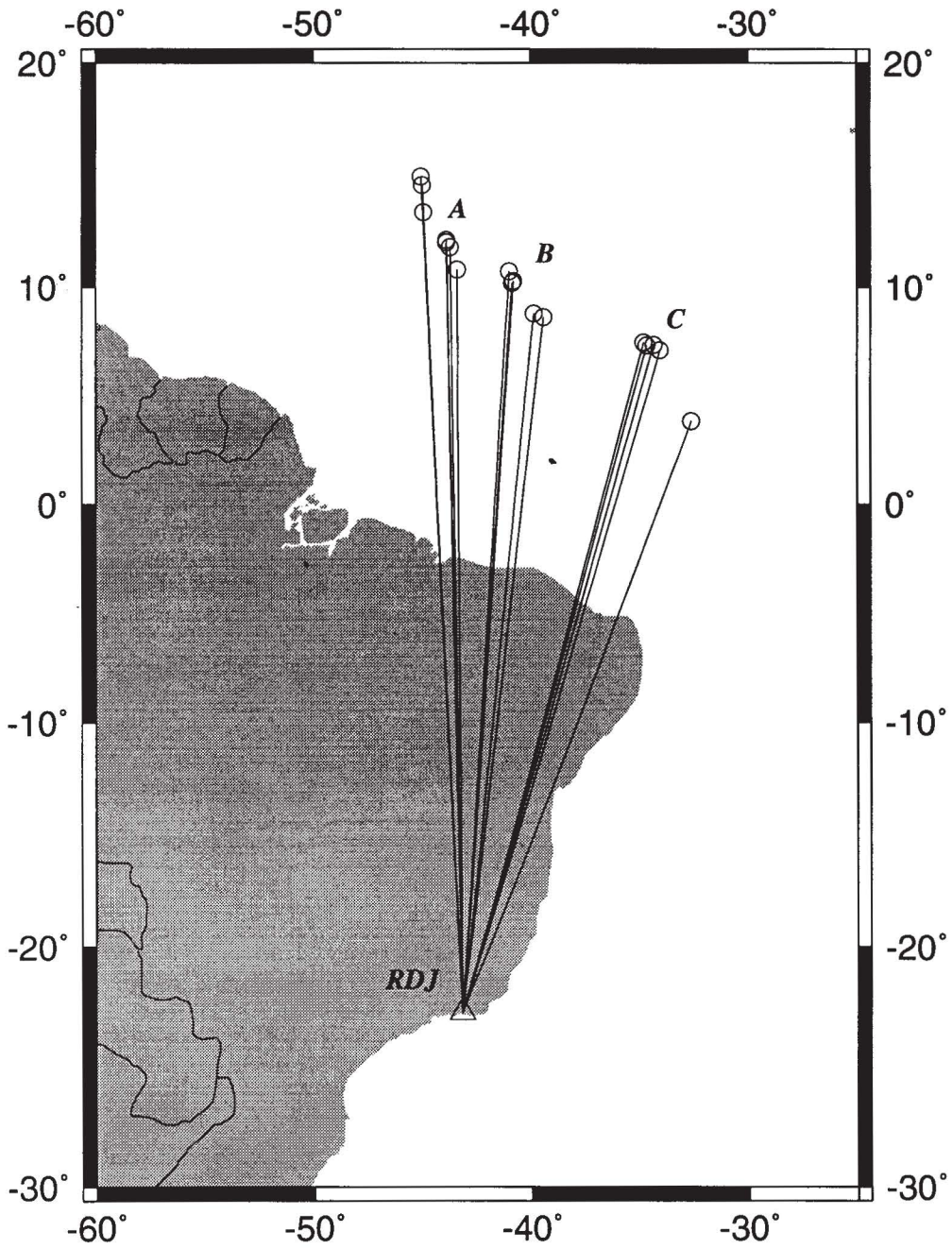

Fig. 1. Map showing both locations of epicenters and station RDJ along with their corresponding source-to-station great circle paths.

study the continental part of the paths it is necessary to make the decomposition of the source-station dispersion curves into oceanic and continental paths. The decomposition process is an old and well known procedure in surface wave studies (Santô, 1960; Santô, 1961, Santô, 1962; Santô, 1963; Santô, 1965; Santô, 1966; Brune and Singh, 1986; Singh, 1988a; Singh, 1988b). Considering that source-station paths are composed of two types of structures, i.e., ocean and continent, then oceanic and continental dispersion curves are related to one another according to the relationship

$$\frac{L_t}{U_t} = \frac{L_c}{U_c} + \frac{L_o}{U_o} \tag{1}$$

where U_t is the group velocity for the mixed oceanic and continental paths, U_c is the group velocity for the pure continental paths, U_o is the group velocity for the pure oceanic path, and L_t, L_c and L_o are lengths of the total, continental and oceanic paths, respectively.

Source-station dispersion curves were computed through the multiple filter technique (Dziewonski *et al.*,

Table 1

Hypocentral parameters of the earthquakes used in this study and corresponding epicentral distances in degrees (deg) and kilometers (km).

event NO.	date Y/M/D	orig. time h min s	latitude deg.	longitude deg.	depth km	magnitudes m_b M_S	epicentral distance deg.	km
1	78/09/11	18 18 22.00 ±0.21 s	10.805 N ±4.78km	43.393 W ±3.22km	33	4.9 4.6	33.54	3729.4
2	79/02/11	08 00 56.50 ±0.16s	10.286 N ±3.77km	40.807 W ±2.79km	10	5.4 5.3	33.06	3676.1
3	79/02/11	09 06 45.00 ±0.18s	10.212 N ±4.23km	40.869 W ±2.42km	10	5.1 4.9	32.98	3667.2
4	79/02/13	01 50 59.60 ±0.12s	12.032 N ±2.68km	43.901 W ±2.03km	10	5.2 4.6	34.72	3860.7
5	79/02/28	08 29 51.90 ±0.50s	12.163 N ±9.66km	43.875 W ±6.05km	10	4.8 4.4	34.85	3875.1
6	79/05/30	16 08 47.20 ±0.12s	14.638 N ±2.93km	45.003 W ±2.02km	10	5.4 5.2	37.34	4152.0
7	79/06/09	06 31 47.00 ±0.13s	11.811 N ±2.92km	43.712 W ±1.62km	10	5.2 4.8	34.49	3835.1
8	80/01/14	17 20 30.20 ±0.51s	7.471 N ±9.98km	34.796 W ±9.71km	10	5.0 —	31.29	3479.3
9	80/07/03	14 40 09.70 ±0.20s	7.361 N ±4.31km	34.338 W ±3.86km	10	4.9 5.0	31.30	3480.4
10	80/07/26	12 53 40.70 ±0.13s	7.102 N ±2.82km	34.044 W ±2.15km	10	5.2 5.3	31.14	3462.6
11	80/08/13	20 46 22.00 ±0.15s	8.800 N ±3.51km	39.870 W ±2.26km	10	5.1 5.2	31.67	3521.5
12	81/03/23	13 19 25.25 ±0.16s	13.396 N ±3.80km	44.945 W ±2.30km	10	5.3 5.4	36.11	4015.3
13	83/03/02	12 06 17.56 ±0.43s	3.841 N ±7.80km	32.602 W ±7.20km	10	5.0 4.9	28.52	3171.3
14	83/10/13	23 27 33.43 ±0.11s	7.331 N ±2.60km	34.662 W ±2.10km	10	5.4 4.7	31.19	3468.2
15	84/01/25	02 46 36.04 ±0.19s	10.735 N ±5.00km	40.995 W ±3.80km	10	4.9 4.6	33.49	3723.9
16	84/01/25	03 51 44.89 ±0.17s	8.644 N ±3.50km	39.414 W ±3.30km	10	5.1 4.8	31.56	3509.3
17	84/05/13	04 05 46.57 ±0.17s	14.997 N ±3.00km	45.055 W ±3.40km	10	4.9 4.5	37.70	4192.1

1969). In order to compute continental dispersion curves from the above equation it is necessary to have an oceanic structure suitable to the region. However, a specific oceanic model for that part of the Atlantic Ocean does not exist in the literature and, therefore, an oceanic model was constructed.

The oceanic model parameters are a combination of several sources of information concerning studies in the Atlantic Ocean. The average thicknesses of both water and sedimentary layers were obtained through charts IA (bathimetry) and VA (depth to basement) for Emery and Uchupi (1984). The thicknesses of the other layers were obtained from Canas and Mitchell (1981). The compressional wave velocities are based on seismic data compilation about the Atlantic Ocean (Emery and Uchupi, 1984). The shear wave velocities of the oceanic model were determined by Canas and Mitchell (1981) for regions of age

older than 65 Ma in the North Atlantic Ocean. The densities for the crust were obtained through the Nafe-Drake relationship (Talwani *et al.*, 1959) and for the upper mantle from Birch's relation (Birch, 1964). This information has been summarized in Table 2.

With the use of an oceanic dispersion curve, obtained from the model of the Table 2, and equation (1), it was possible to calculate the seventeen pure continental dispersion curves.

Table 2

Earth model used to remove oceanic part of the mixed paths. α is compressional wave velocity, β is shear wave velocity and ρ is density.

thickness (km)	α (km/s)	β (km/s)	ρ (g/cm^3)
4.4	1.52	0.00	1.03
1.6	2.10	1.00	2.10
5.4	6.70	3.80	3.00
48.5	8.10	4.54	3.32
165.0	7.80	4.45	3.21
∞	8.40	4.72	3.43

As can be seen in Figure 1, the geographical distribution of the epicenters suggested the formation of three groups of paths (A, B and C). Group A is composed of seven earthquakes, while both B and C are composed of five earthquakes (Figure 1). Three continental dispersion curves, one for each path (Table 3), were computed through a Chebyshev polynomial fit (Dean, 1986). These dispersion curves will be used in the next section to obtain the shear wave velocity structure for each path.

Errors in group velocity measurements have been widely discussed in the literature. Chave (1979) and Cloetingh *et al.* (1979) have discussed these errors. Determinations of group velocities are commonly affected by several factors such as epicentral mislocation, origin time, source finiteness, initial phase in the source, rise time, etc. In this study, all errors in the continental dispersion curves were calculated assuming that epicenters are located at the intersection between the Rayleigh wave paths and the continental-ocean boundary (Figure 1). The dispersion curve representative of path C was used to show the effects of these errors on group velocities measurements. This path was considered because it has the lowest continental distance and therefore the highest group velocity errors.

Although the uncertainties in the epicentral distances are lower than 10 km (Table 1), an uncertainty of ±20 km has been considered in the calculation of this error. This has produced group velocity variation from 0.018 to 0.022 km/s. In a similar way, an uncertainty of 2s was used to calculate the influence of origin time in group velocity measurements. This produces group velocity uncertainties varying from 0.005 to 0.008 km/s. Source finiteness error produces an error of 3s (Kanamori, 1970) and, therefore, group velocity errors from 0.008 to 0.012 km/s. Initial phase in the source has an uncertainty of 2s and a group velocity error which varies from 0.005 to 0.008 km/s. Rise time errors have a time variation of 1s, and, therefore, group velocity errors varying from 0.002 to 0.004 km/s. With the use of the estimates described above it was possible to compute the total error for each period component through the root mean square sum of the errors owing to epicenter mislocation, earthquake origin time, source finiteness, initial phase in the source, rise time, and standard deviations of the Chebyshev polynomial fit. These total errors are shown in Table 3.

INVERSION OF RAYLEIGH WAVE GROUP VELOCITIES

A mentioned in the introduction, the crustal and upper mantle structures of the Brazilian territory have been little investigated due essentially to the low density distribution of seismological stations. In spite of this, it is possible to find in the literature regional surface wave studies in this area.

The parametrization used in this study is based on a survey developed by Hwang and Mitchell (1987). They split the South American continent into eastern and western parts to investigate the S-wave velocities and Q in both regions and compared their results with others found in regions of similar geological and tectonic characteristics.

A differential inversion method implemented in the computer program SURF (Herrmann, 1991) was used to obtain the shear wave velocity structure of the eastern part of the Brazil. The shear wave velocity structure for the eastern part of South American continent (Hwang and Mitchell, 1987) was used as the starting model.

The inversion procedure was divided into two steps. In the first step, the starting model, containing many thin layers overlying an infinite half-space, is inverted and the resulting shear wave velocity structure is used to make another parametrization. The resolving kernels of the first step are also useful to define the next model. In the second step, groups of thin layers with similar characteristics are transformed into thicker layers and the new starting model is again inverted. The results of these procedures will be shown and discussed in the next section.

DISCUSSION AND INTERPRETATION

The results for the first step of the inversion for each path are shown in Figures 2-4. The predicted and observed Rayleigh wave group velocities are shown in Figures 2a, 3a and 4a, while the estimated shear wave velocity structures and corresponding resolving kernels are displayed in Figures 2b, 3b and 4b.

In the crust, all models show strong velocity gradients at 10, 20 and 40 km, which were introduced with the start–

Table 3

Experimental Rayleigh wave group velocities (U) for each path (A, B and C) obtained after correction of the oceanic patn and application of a Chebyshev polynomial fit. The total errors, discussed in the text, are also shown.

	PATH A		PATH B		PATH C	
T(s)	U (km/s)	e (km/s)	U (km/s)	e (km/s)	U (km/s)	e (km/s)
20.1	3.028	± 0.027	3.089	± 0.029	3.188	± 0.031
21.3	3.038	0.027	3.081	0.029	3.211	0.031
23.3	3.091	0.027	3.105	0.029	3.272	0.032
25.0	3.155	0.028	3.149	0.030	3.331	0.037
26.9	3.233	0.029	3.213	0.032	3.395	0.033
29.3	3.331	0.031	3.302	0.032	3.466	0.040
30.1	3.361	0.031				
31.0	3.393	0.032	3.364	0.033	3.507	0.036
33.0	3.458	0.032	3.433	0.034	3.549	0.035
34.1	3.490	0.032				
35.3	3.521	0.033	3.502	0.034	3.588	0.036
36.6	3.553	0.033			3.608	0.036
37.9	3.581	0.034	3.567	0.035	3.626	0.036
39.4	3.612	0.034	3.598	0.037	3.646	0.036
41.0	3.642	0.035	3.626	0.036	3.666	0.037
42.7	3.673	0.037	3.652	0.037	3.686	0.039
44.5	3.705	0.036	3.675	0.045	3.705	0.037
46.5	3.739	0.053	3.697	0.047	3.723	0.038
48.8	3.777	0.038	3.719	0.039	3.738	0.039
51.2	3.813	0.078	3.740	0.039	3.735	0.071
53.9	3.845	0.040			3.746	0.039
56.9	3.864	0.076	3.790	0.040	3.751	0.040
60.2	3.866	0.044	3.820	0.041	3.755	0.040
64.0	3.869	0.121	3.854	0.048	3.759	0.047
68.3			3.887	0.045	3.767	0.043
73.1	3.875	0.069	3.910	0.067	3.775	0.049
78.8			3.912	0.047	3.780	0.053
85.3	3.881	0.075	3.900	0.057	3.785	0.048
93.1			3.903	0.054		
102.4	3.887	0.089	3.892	0.054	3.795	0.066
113.8			3.899	0.080		

ing model. Only the crustal shear wave velocity structure of path A exhibits any similarity with the shear wave velocity structure of Hwang and Mitchell (1987). The resolving kernels for the upper crust (20 km thickness) were very poor (Figures 2b, 3b and 4b). Reasonable resolving kernels were obtained only for the lower part of the crust (Figures 2b, 3b and 4b). Below the Moho, which is characterized by shear wave velocities around 4.4 km/s and lying at depths of 40 km (Figures 2b, 3b and 4b), the models corresponding to both paths A and B present, in general, similar behavior. The low velocity zone, between 150 and 250 km depth, is not well defined in paths A and B. It is a little pronounced only in path A. Meanwhile, the resolving kernels for those layers were poor and, therefore, it is difficult

(A)

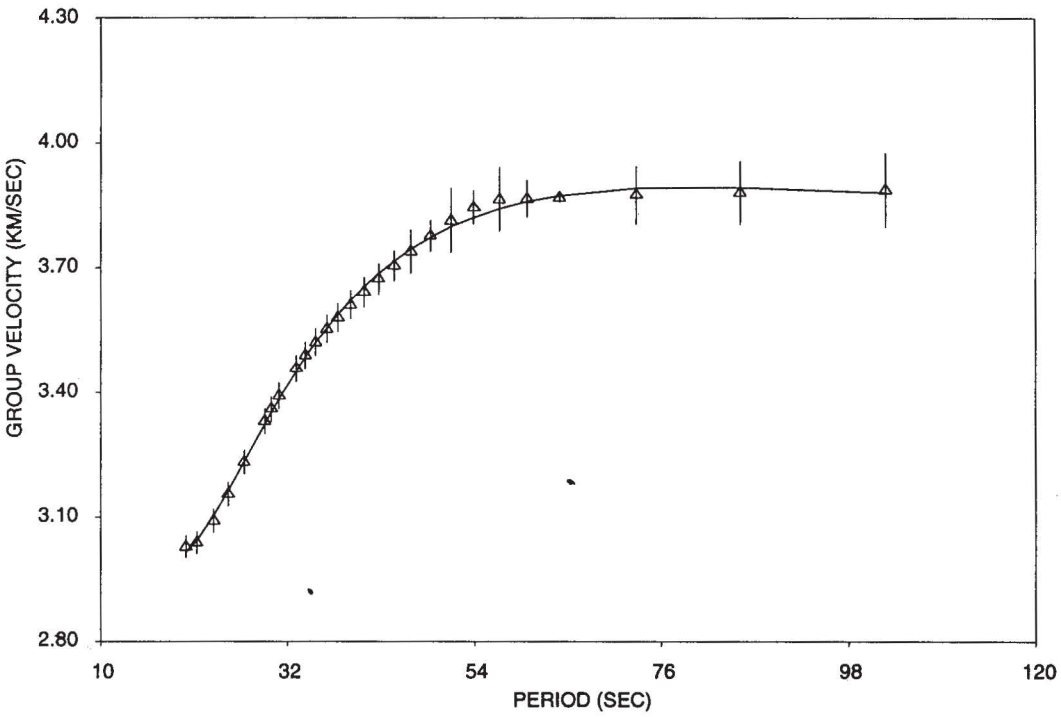

(B)

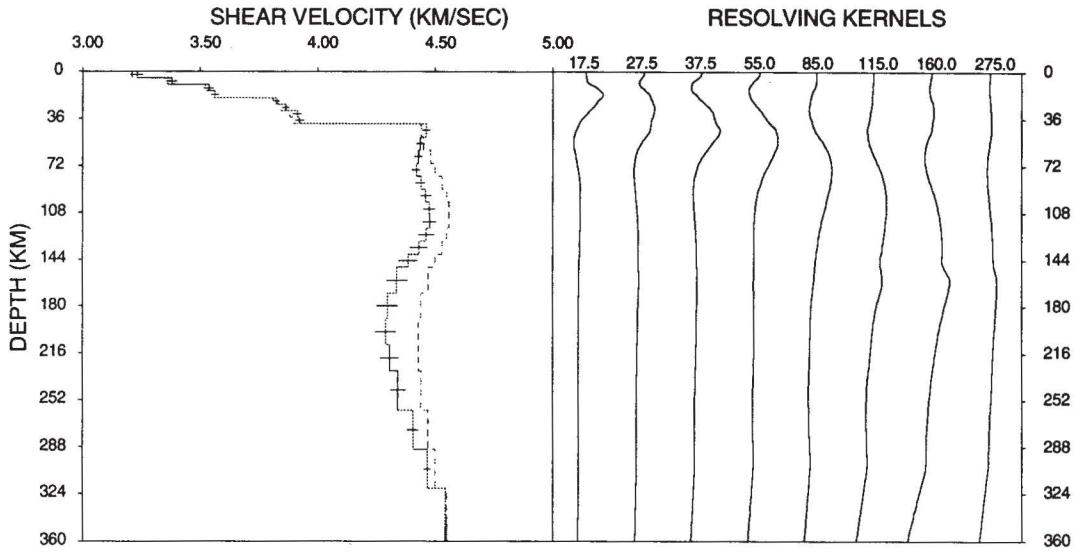

Fig. 2. First inversion results for path A. A damping parameter of 0.05 was used in the inversion process. (a) Experimental (triangles) and theoretical (solid line) Rayleigh wave group velocities. Vertical bars on the triangles are total errors as discussed in the text. (b) On the left side are shown both estimated shear wave velocity structure (solid line) with its corresponding standard deviation (horizontal bars), and the starting model (dashed line). In the right side are displayed the resolving kernels at selected layers.

to make any definite conclusions about the structure. Path C inversion results show a faster decrease of the shear wave velocity with depth below the crust-mantle transition, which could be associated with a thinner lithosphere. As in other paths the resolution at these depths is not good enough for definite conclusions.

As described in the previous section, these results were used to define other starting models. These new starting models were defined and a new inversion was developed. The results of the new inversion are shown in Figures 5-7 and Table 4. The theoretical and observed Rayleigh wave group velocities are shown in Figures 5a, 6a and 7a. The

(A)

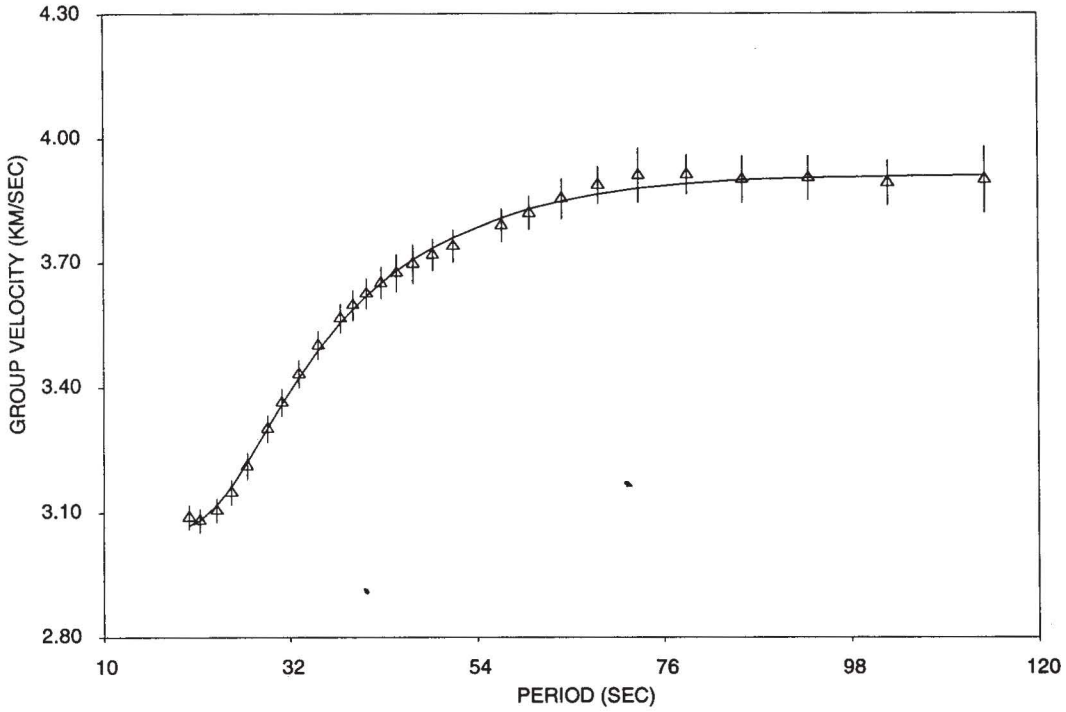

(B)

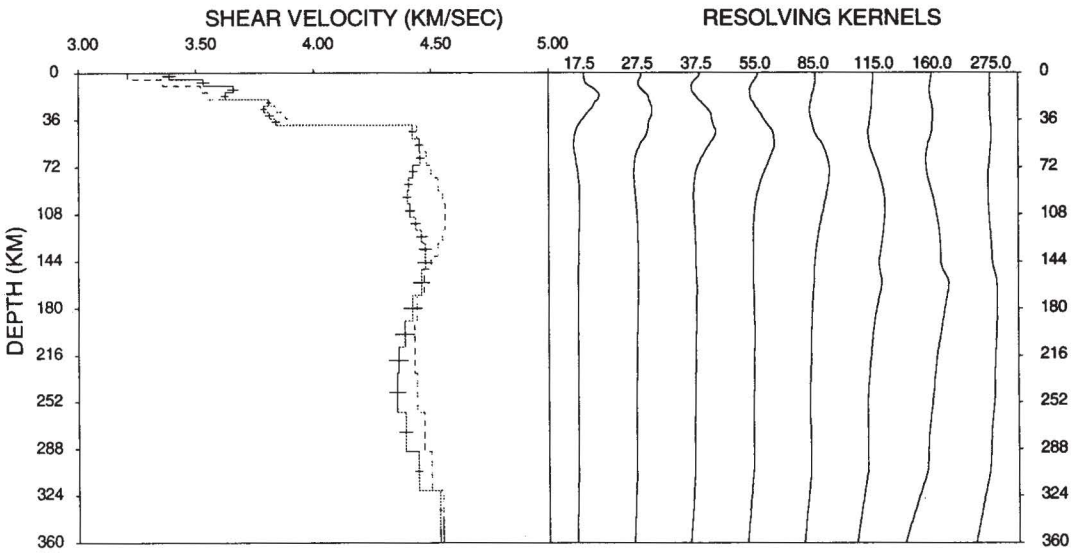

Fig. 3. First inversion results for path B. A damping parameters of 0.05 was used in the inversion process. (a) Experimental (triangles) and theoretical (solid line) Rayleigh wave group velocities. Vertical bars on the triangles are total errors discussed in the text. (b) On the left side are shown both estimated shear wave velocity structure (solid line) with its corresponding standard deviation (horizontal bars), and the starting model (dashed line). In the right side are displayed the resolving kernels at selected layers.

estimated shear wave velocity structures and corresponding resolving kernels are shown in Figures 5b, 6b and 7b.

As in the first step, all models show velocity gradients at 10, 20 and 40 km depth and only the shear wave velocity structure of path A is similar to the starting model (Figure 5b). The worst resolution in the crust is concentrated in the upper layer (10 km thickness) where β has assumed an average value of 3.43 km/s (Table 4). The intermediate and lower parts of the crust exhibit good resolution in all models (Figures 5b, 6b and 7b), and have average β values of 3.58 and 3.85 km/s, respectively (Table 4).

The sub-Moho layer has almost the same shear wave

(A)

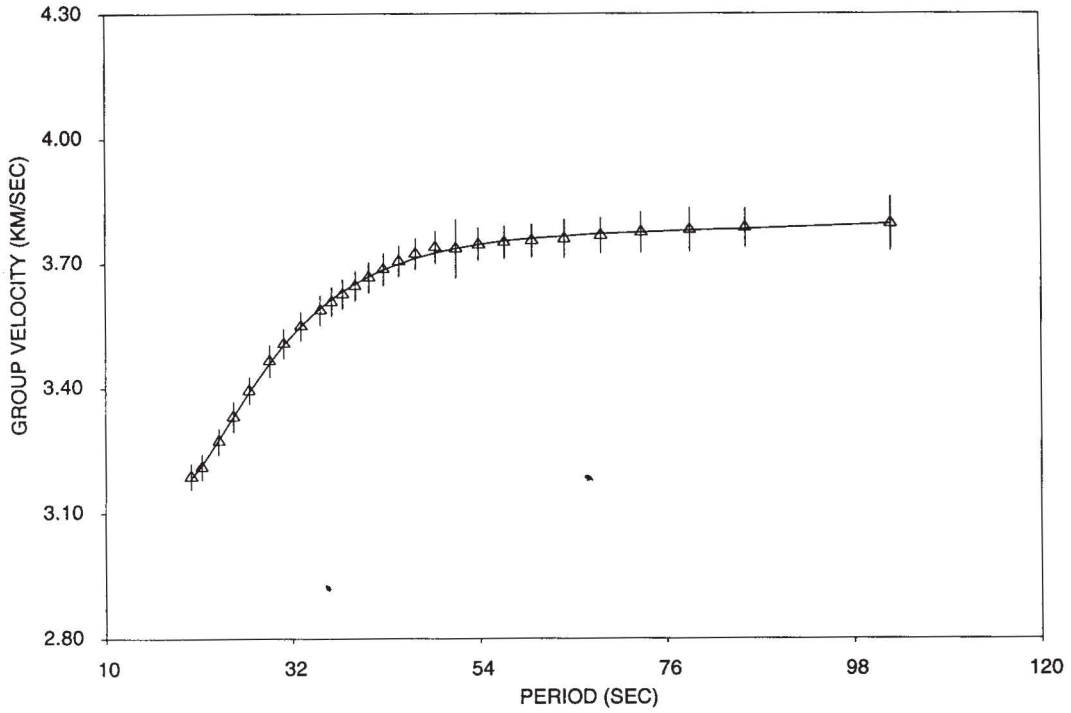

(B)

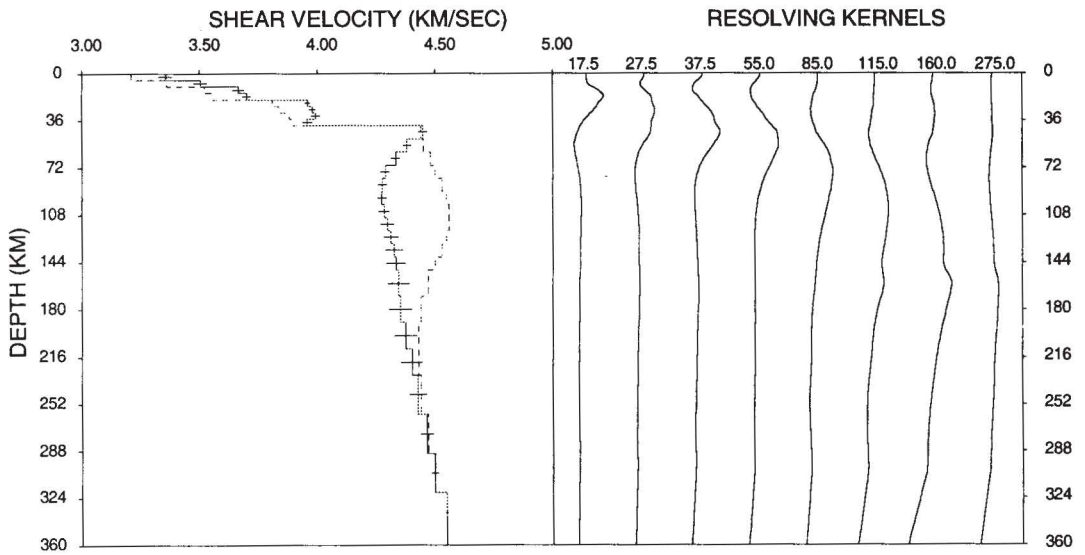

Fig. 4. First inversion results for path C. A damping parameters of 0.05 was used in the inversion process. (a) Experimental (triangles) and theoretical (solid line) Rayleigh wave group velocities. Vertical bars on the triangles are total errors discussed in the text. (b) On the left side are shown both estimated shear wave velocity structure (solid line) with its corresponding standard deviation (horizontal bars), and the starting model (dashed line). In the right side are displayed the resolving kernels at selected layers.

velocity value for both paths A and B (4.43 km/s and 4.41 km/s), but with different thicknesses (Table 4). The shear wave velocity is a little lower in path C (4.36 km/s). The most important aspect observed in that layer is the good resolution for all models (Figures 5b-7b).

Below the sub-Moho layer, it is possible to observe a layer of low velocity with an average shear wave velocity of 4.28 km/s (Table 4). In path A, it is between 150 and 260 km depth, but it has a large uncertainty and poor resolution (Figure 5b). Resolution of the estimated parameter can be analyzed through spread of the resolving kernel (i.e., a large spread is related to poor resolution of the parameter, while a short spread is associated with good resolution). In

(A)

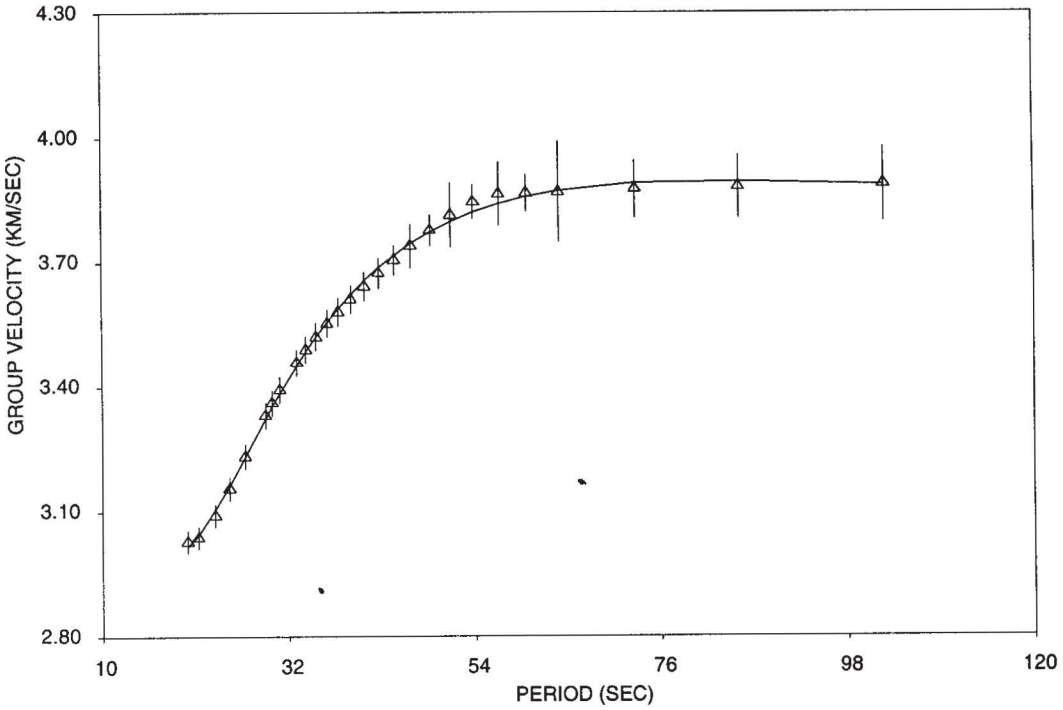

(B)

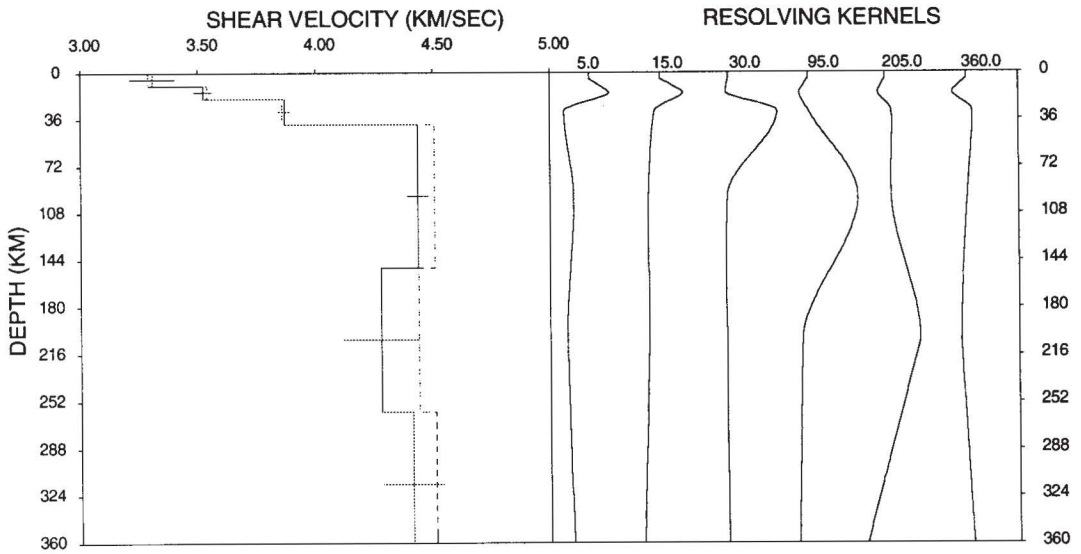

Fig. 5. Final inversion results for path A. A damping parameters of 0.01 was used in the inversion process. (a) Observed (triangles) and theoretical (solid line) Rayleigh wave group velocities. Vertical bars on the triangles are total errors discussed in the text. (b) On the left side are shown both estimated shear wave velocity structure (solid line) with its corresponding standard deviation (horizontal bars), and the starting model (dashed line). In the right side are displayed the resolving kernels associated with each layer of the model.

path B this zone does not seems to be clear and it also has a large spread and, therefore, poor resolution (Figure 6b). The best resolution for this layer is observed only in path C (Figure 7b).

In the half-space all models show a poor resolution and an average shear wave velocity of 4.35 km/s. The maximum depth for the model of path C was reduced because there was no difference between the low velocity zone and the lower layers and, therefore, a half-space was the better representation.

The models analyzed above were also compared with six other models representing four Precambrian shield areas

(A)

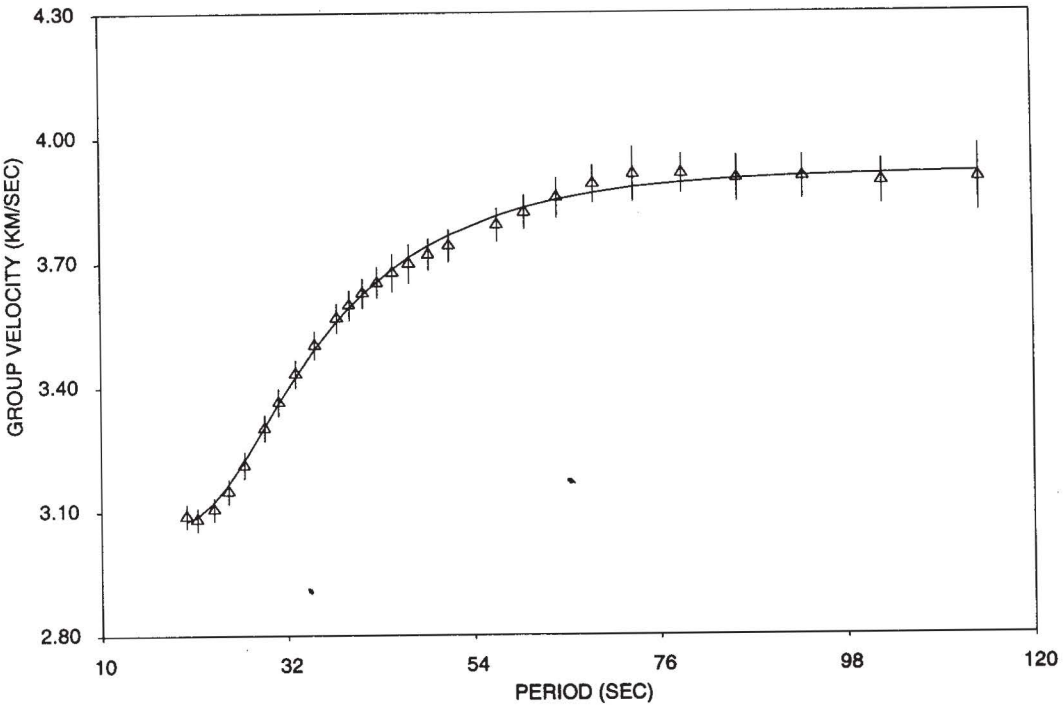

(B)

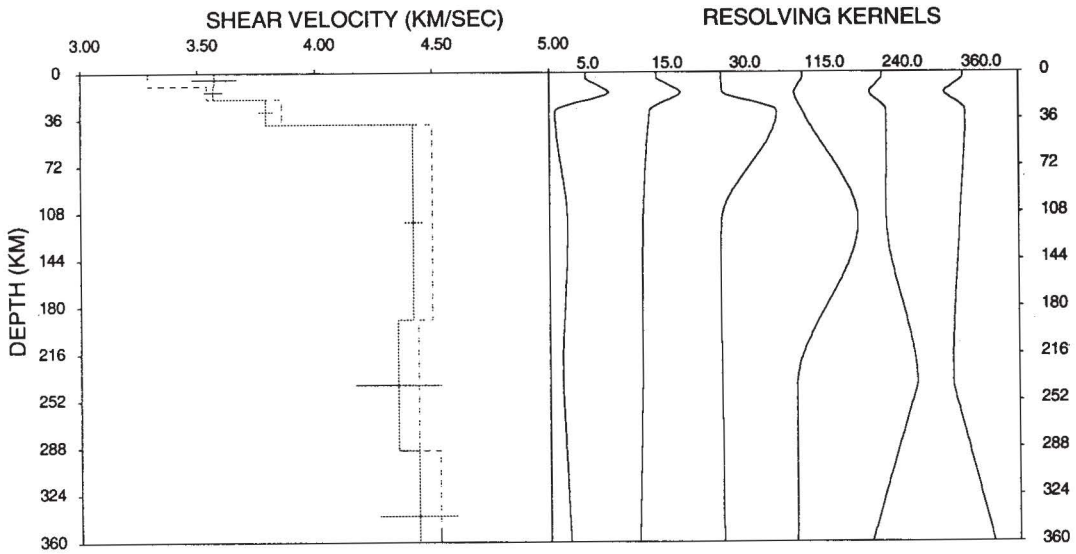

Fig. 6. Final inversion results for path B. A damping parameter of 0.01 was used in the inversion process. (a) Observed (triangles) and theoretical (solid line) Rayleigh wave group velocities. Vertical bars on the triangles are total errors discussed in the text. (b) On the left side are shown both estimated shear wave velocity structure (solid line) with its corresponding standard deviation (horizontal bars), and the starting model (dashed line). In the right side are shown the resolving kernels associated with each layer of the model.

(Figure 8). These models are: CANSD (Canadian shield-Brune and Dorman, 1963), AFRIC (African shield-Gumper and Pomeroy, 1970), A-1 (Antarctic shield-Dewart and Toksoz, 1965), eastern Antarctica and western Antarctica (Singh, 1994) and eastern South America (Hwang and Mitchell, 1987).

In the crust, mainly the upper part, all models are very close to one another and, therefore, no significant variation is observed. In the lower crust, between 17 and 35 km depth, the models show a larger scatter. However, the principal differences occur below the Moho. From 40 to 70 km depth, the models obtained in the present study show an

(A)

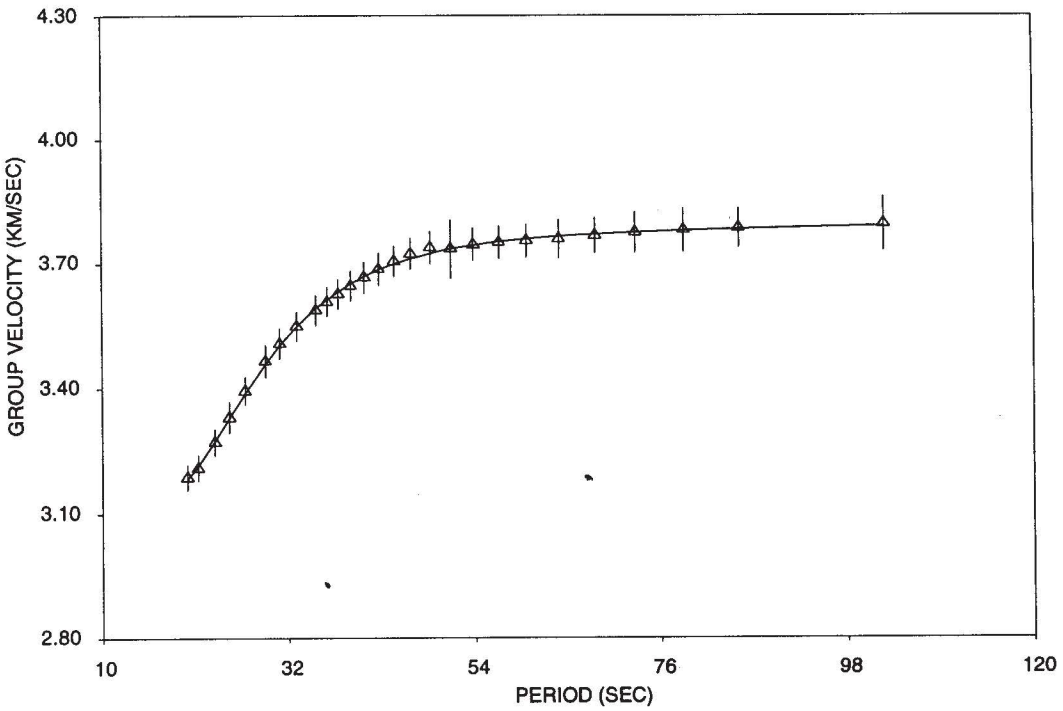

(B)

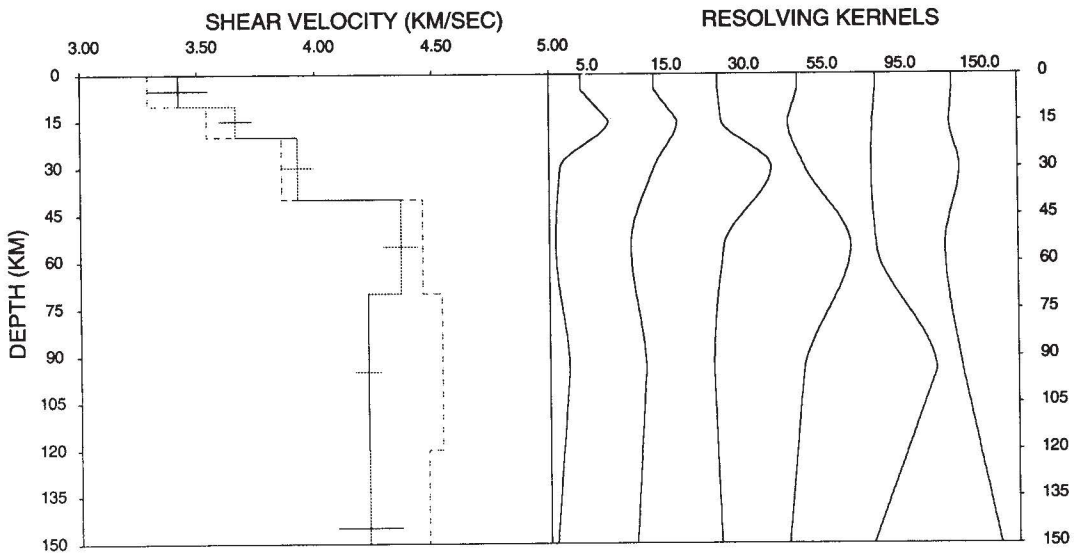

Fig. 7. Final inversion results for path C. A damping parameters of 0.01 was used in the inversion process. (a) Observed (triangles) and theoretical (solid line) Rayleigh wave group velocities. Vertical bars on the triangles are total errors discussed in the text. (b) On the left side are shown both estimated shear wave velocity structure (solid line) with its corresponding standard deviation (horizontal bars), and the starting model (dashed line). In the right side are shown the resolving kernels associated with each layer of the model.

excellent agreement with both the A-1 model and the eastern South America model, as well as a good agreement with both the eastern and western Antarctica models from Singh (1994). The Canadian and African models are in complete disagreement with the others models. The similarity between the models described above can be extended down to 150 km depth (Figure 8). Below this depth only the model for path B (Figure 8) shows any similarity with the others models. The Canadian model shows similarity with the eastern South America model only in the depth

Table 4

Estimated shear wave velocity structures for paths A, B and C. β is shear wave velocity and σ is the standard deviation.

PATH A			PATH B			PATH C		
thickness (km)	β (km/s)	σ (km/s)	thickness (km)	β (km/s)	σ (km/s)	thickness (km)	β (km/s)	σ (km/s)
10.0	3.30	0.10	10.0	3.57	0.09	10.0	3.42	0.13
10.0	3.52	0.04	10.0	3.56	0.04	10.0	3.66	0.07
20.0	3.86	0.03	20.0	3.79	0.03	20.0	3.92	0.07
110.0	4.43	0.04	150.0	4.41	0.04	30.0	4.36	0.07
110.0	4.27	0.16	100.0	4.35	0.18	50.0	4.22	0.05
∞	4.41	0.13	∞	4.43	0.17	∞	4.22	0.14

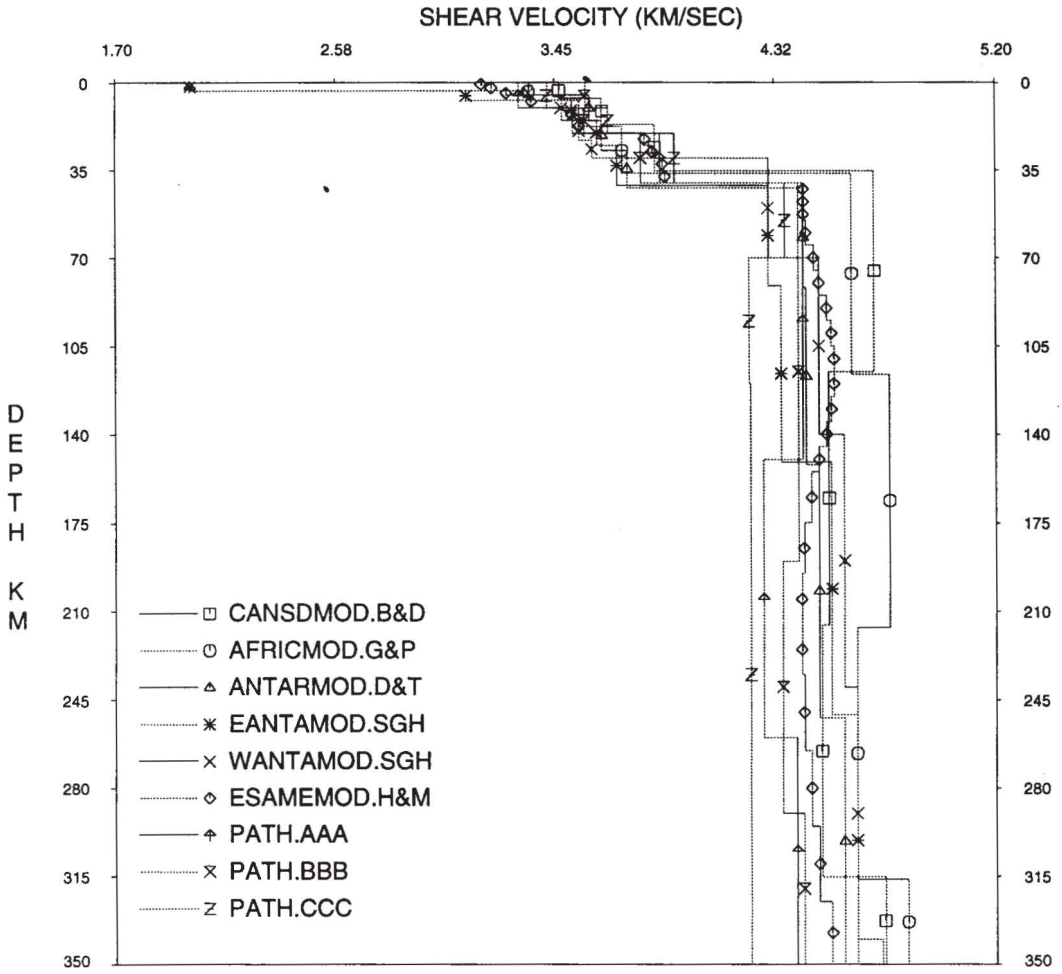

Fig. 8. Comparison between the estimated shear wave velocity structures obtained in this study and several Earth models representative of shield areas. The symbol for each model is indicated at the lower left. CANSDMOD.B&D is Canadian's model (Brune and Dorman, 1963). AFRICMOD.G&P is African's model (Gumper and Pomeroy, 1970). ANTARMOD.D&T is Antarctica's model (Deward and Toksoz, 1965). EANTAMOD.SGH and WANTAMOD.SGH are Antarctica's model (Singh, 1994). ESAMEMOD.H&M is eastern South America's model (Hwang and Mitchell, 1987). The models PATH.AAA, PATH.BBB and PATH.CCC are those obtained in the present study (Table 4). It should be noted between the top of the sub-Moho layer and 150 km depth the models PATH.AAA, PATH.BBB and ANTARMOD have practically the same shear wave velocities, and Antarctica models EANTAMOD and WANTAMOD are close to these models.

range from 150 to 315 km. The African model did not present any correlation with the other models in the depth range from 35 to 250 km (Figure 8). Between 120 and 250 km depth, the eastern South America model, which represents far-flung paths across Brazilian territory, also shows good agreement with all the models of Antarctica. At a

glance, the similarity between models of Antarctica and of Brazil is probably related to the past existence of Gondwanaland.

CONCLUSION

The S wave velocity structure of the eastern part of Brazil has been obtained through Rayleigh wave dispersion curves obtained at the Brazilian seismological station RDJ. Seventeen earthquakes which occurred in the North Atlantic Ocean were divided into three groups of paths (A, B and C) and a surface wave dispersion curve representative of each path was calculated. The inversion results of these dispersion curves show that the crustal structure is composed of three layers with S wave velocities varying from 3.30-3.57 km/s, 3.52-3.66 km/s and 3.86-3.92 km/s, respectively. The sub-Moho layer is characterized by shear wave velocities varying from 4.41 to 4.43 km/s. Path C exhibits a sub-Moho thickness thinner that the other paths. Low velocity zones, characterized by shear wave velocities of 4.27 and 4.22 km/s, are observed in both paths A and C, but is clearly resolved only in path C where the shear wave velocity is 4.22 km/s. A comparative analysis between the models obtained in the present study and those representative of others shield areas reveals a similarity between the Brazilian, eastern South American and Antarctica models; this seems to be correlated with the past existence of the Gondwanaland.

ACKNOWLEDGMENTS

The author would like to thank CNPq/Observatório Nacional for financial support to take part in the Regional Seismological Assembly in South America.

BIBLIOGRAPHY

BIRCH, F., 1964. Density and composition of mantle and core. *J. Geophys. Res., 69*, 4377-4388.

BRUNE, J. and J. DORMAN, 1963. Seismic waves and earth structure in the Canadian shield. *Bull. Seism. Soc. Am., 53*, 167-210.

BRUNE, J. N. and D. D. SINGH, 1986. Continent-like crustal thickness beneath the Bay of Bengal sediments. *Bull. Seism. Soc. Am., 76*, 191-203.

CANAS, J.A. and B.J. MITCHELL, 1981. Rayleigh wave attenuation and its variation across the Atlantic Ocean. *Geophys. J. R. Astr. Soc., 67*, 159-176.

CHAVE, A.D., 1979. Lithospheric structure of the Walvis ridge from Rayleigh wave dispersion. *J. Geophys. Res., 84*, 6840-6848.

CLOETINGH, S., G. NOLET and R. WORTEL, 1979. On the use of Rayleigh wave group velocities for the analysis of continental margins. *Tectonophysics, 59*, 335-346.

DEAN, E. A., 1986. The simulataneous smoothing of phase and group velocities from multi-event surface wave data. *Bull. Seism. Soc. Am., 76*, 1367-1383.

DEWART, G. and M. TOKSOZ, 1965. Crustal structure in east Antarctica from surface wave dispersion. *Geophys. J. R. Astr. Soc., 10*, 127-139.

DZIEWONSKI, A., S. BLOCH and M. LANDISMAN, 1969. A technique for the analysis of transient seismic signals. *Bull. Seism. Soc. Am., 59*, 427-444.

EMERY, K. O. and E. UCHIPI, 1984. The geology of the Alantic Ocean, Springer-Verlag, New York.

GUMPER, F. and P.W. POMEROY, 1970. Seismic wave velocity and earth structure on the African continent. *Bull. Seism. Soc. Am., 60*, 651-668.

HERRMANN, R.B., 1991. Computer programs for Seismology, vol. IV, St. Louis University, St. Louis, MO.

HWANG, H.-J. and B. J. MITCHELL, 1987. Shear velocities, Q_β, and the frequency dependence of Q_β in stable and tectonically active regions from surface wave observations. *Geophys. J. R. Astr. Soc., 90*, 575-613.

KANAMORI, H., 1970. The Alaska earthquakes of 1964: Radiation of long-period surface waves and source mechanism. *J. Geophys. Res., 75*, 5029-5040.

SANTÔ, T. A., 1960. Observation of surface waves by Columbia-type seismograph installed at Tsukuba station, Japan (Part I)-Rayleigh wave dispersions across the oceanic basin. *Bull. Earth. Res. Inst., 38*, 219-240.

SANTÔ, T. A., 1961. Rayleigh wave dispersions across the oceanic basin around Japan (Part III)-On the crust of the south-western Pacific Ocean. *Bull. Earth. Res. Inst., 39*, 1-22.

SANTÔ, T. A., 1962. Dispersion of surface waves along various paths to Uppsala, Sweden. Part I: Continental paths. *Ann. Geofis., 15*, 245.

SANTÔ, T. A., 1963. Division of the Pacific area into seven regions in each of which Rayleigh have the same group velocities. *Bull. Earth. Res. Inst., 41*, 719.

SANTÔ, T. A., 1965. Lateral variation of Rayleigh wave dispersion character. Part I: Observational data. *Pure and Appl. Geophys., 62*, 49.

SANTÔ, T. A., 1966. Lateral variation of Rayleigh wave dispersion character. Part III: Atlantic Ocean, Africa and Indian Ocean. *Pure and Appl. Geophys., 63*, 40-59.

SINGH, D. D., 1988a. Crust and upper-mantle velocity structure beneath the northern and central Indian Ocean from the phase and group velocity of Rayleigh and Love waves. *Phys. Earth. Planet. Inter., 50,* 230-239.

SINGH, D. D., 1988b. Quasi-continental oceanic structure beneath the Arabian Fan sediments from observed surface-wave dispersion studies. *Bull. Seism. Soc. Am., 78,* 1510-1521.

SINGH, D. D., 1994. Shear-wave velocity and attenuation structure beneath Antarctica determined from surface waves. *Geophys. J. Int., 118,* 515-528.

TALWANI, M., G. H. SUTTON and J. L. WORZEL, 1959. A crustal section across the Puerto Rico Trench. *J. Geophys. Res., 64,* 1545-1555.

Jorge Luis de Souza
Observatório Nacional, Departamento de Geofísica,
R. Gal. José Cristino, 77-São Cristovão,
20921-400 Rio de Janeiro, Brasil.